Ratio Mathematica Volume 54, 2025

The Bayesian Hidden Markov Chain Modeling of the Ghana COVID-19 Blood Type Infection Distribution

Joseph Johnson Kwabina Arhinful*
Emmanuel deGraft Johnson Owusu-Ansah†
Adebanji Atinuke ‡
Accam Bennet §

Abstract

This study uses Hidden Markov Chain (HMC) analysis to explore how blood type influences infection progression and recovery probabilities. The results show significant differences between blood types. Individuals with blood type O^+ have higher transition probabilities from severe to milder infection states, especially from state $[5, 1]$ to $[1, 1]$ with a probability of 0.3634, indicating a better likelihood of recovery. In contrast, O^- individuals are more likely to remain in severe states, with a transition probability of 0.5132 from state $[1, 1]$ to itself, suggesting prolonged illness. Blood types A^+ and A^- generally show stability, with higher recovery probabilities for A^+. For B^+ and B^-, early intervention is crucial, with favorable outcomes suggested by transition probabilities. AB^+ and AB^-were more stable and less infectious group. Overall, blood type influences disease progression, highlighting the need for personalized treatment strategies.

Keywords: Hidden Markov Chain; Bayesian-Poisson Hidden Markov; COVID-19; Transition Probabilities

2020 AMS subject classifications: 62C10 [1]

*Statistics and Actuarial Science, Kwame Nkrumah Univ. of Sci. & Tech. (KNUST) Ghana, Takoradi Technical University, Ghana; johnsonjoseph83@yahoo.com.

†Statistics & Actuarial Science, KNUST Ghana; edjowusu-ansah.cos@knust.edu.gh.

‡Statistics & Actuarial Science, KNUST Ghana, aoadebanji.cos@knust.edu.gh

§Statistics & Actuarial Science, KNUST Ghana, barneytotos@hotmail.com

[1]Received on May 17, 2024. Accepted on December 5, 2024. Published on March 24, 2025.
DOI:10.23755/rm.v54i0.1602. ISSN 1592-7415; e-ISSN 2282-8214.

1 Background

The rapid spread and varying clinical outcomes of COVID-19 are continuing to highlight the importance of identifying factors that are influencing disease susceptibility, progression, and recovery. Among these factors, blood types are attracting attention for their potential role in modulating the risk and severity of infection. Researchers are currently suggesting associations between specific blood types and susceptibility to COVID-19, yet the mechanisms underlying these associations are remaining unclear. This is opening an opportunity for advanced modeling techniques to explore these relationships and provide robust, data-driven insights (Mielke N [2024]).

Hidden Markov Models (HMMs) are offering a powerful framework for studying the progression of infectious diseases, particularly when direct observations of health states are remaining challenging. HMMs are being used to capture temporal dynamics and stochastic transitions between latent states—such as susceptibility, infection, and recovery—that are playing a crucial role in disease progression. By incorporating observable markers such as blood types, HMMs are quantifying their influence on these transitions and are providing a probabilistic understanding of the disease's underlying processes (Sarode Rekha [2023]).

Hidden Markov Chains (HMMs) are strong probabilistic models that explain sequences of observable events by assigning each event to an underlying unobservable state (Raffa [2012], Nam et al. [2014],Koerniawan et al. [2020]). These models have a wide range of applications, including voice recognition, bioinformatics, natural language processing, finance, and other areas of importance to researchers (Luo et al. [2014]). In a Hidden Markov Chain, the underlying process progresses through a series of states, but the states themselves are not readily visible (Song et al. [2018]). Instead, an observation or measurement is performed at each time step based on the probability of the present underlying condition. The sequence of observations gives indirect information on the sequence of underlying states, and the purpose is to determine the most probable sequence of states based on the observed data (Castillo-Riquelme et al. [2008]). One of the main components of HMC is the Markov property, which asserts that the likelihood of transitioning to a certain state is determined only by the present state and not by the sequence of events that preceded it. This trait simplifies the modeling process and enables the efficient calculation of probabilities inside the model (Ackermann et al. [2019]). The HMC generally has three sets of parameters: starting state probabilities, state transition probabilities, and emission probabilities. The starting state probabilities reflect the probability distribution of the concealed states

DOI:10.23755/rm.v53i0.1602. ISSN: 1592-7415. eISSN: 2282-8214.

at the start of the series (Alafchi et al. [2018]). The state transition probabilities indicate the chance of moving from one concealed state to another. Finally, emission probabilities indicate the chances of seeing a certain event given a concealed state.

A Bayesian method for modeling HMMs uses a probabilistic framework to estimate model parameters and make predictions. Bayesian approaches provide more robust inference by including previous information about the parameters into the model, which is especially useful when data is limited or noisy (King et al. [2016]). The Bayesian Poisson Markov Chain (BPMC) is a special variation of the Hidden Markov Chain. In BPMCs, observations are assumed to follow a Poisson distribution, while underlying states change using a Markovian process. BPMCs are especially effective for modeling count data, which is concerned with the number of occurrences of an event over a certain time or space period (Su and Wang [2020]). Prior distributions are allocated to model parameters in BPMC based on known or perceived values. These priors are subsequently updated with observed data, yielding posterior distributions that include both prior knowledge and empirical evidence (Rojas-Salazar et al. [2020]). In comparison to standard frequentist approaches, this Bayesian approach enables more robust and flexible modeling.

In this study, HMMs is used to investigate the role of blood types in the progression of COVID-19. Specifically, HMMs are enabling the integration of multivariate data, including blood types and clinical indicators, to infer latent health states and transition probabilities. By doing so, this approach is enhancing our understanding of the relationship between blood types and COVID-19 outcomes while demonstrating the broader applicability of HMMs in personalized diagnostics and disease modeling. Specifically, the study seeks to estimate the transmission and infection rates among the blood types and go into the complexities of the transition probability estimation process, explaining the approaches used and the insights gained. Moreover, to uncover the latent dynamics contained inside the hidden Markov model using actual data and robust statistical approaches and understand the transitions within the stages to explain the stages of the infection. The study's investigation into Hidden Markov Chains goes beyond theoretical abstractions, attempting to bridge the gap between seen data and underlying processes, helping to reveal the underlying transitions of COVID-19 infection in the face of blood types and rhesus factors, by revealing the estimated transition probabilities inside the hidden Markov model, hence, the study intends to provide a thorough knowledge of the blood system's behavior, opening the way for informed decision-making and predictive modeling in dealing with pandemics.

2 Related Works

2.1 The Hidden Markov Chain and Models

The Hidden Markov Chain (HMC) model has been widely explored and implemented in many domains, including voice recognition, bioinformatics, and finance. Baum and colleagues introduced the HMC in the 1960s (Sarode Rekha [2023], Baum L. E. [1966]), a probabilistic model used to study sequences of observable data. The model assumes that the underlying Markov process has unobservable states. The model is made up of two primary components: the hidden states, which develop via a Markov process, and the observable emissions, which are dependent on the underlying hidden states. R. [1989] pioneered the use of HMC for voice recognition problems. Rabiner proved the HMC's usefulness in modeling sequential data, notably voice signals, by taking advantage of the data's intrinsic temporal relationships. In bioinformatics, HMC has been used to solve a variety of issues, including gene prediction, protein structure prediction, and sequence alignment (Gang Q [2024], Johnson and Willsky [2013]). Other works, which has seen the HMM applications include financial time series (Zhang Y. [2019]), voice and hand writing recognitions(Li Y. [2016]). It has been established that, the utility of HMMs in modeling continuous physiological signals, such as EEG, ECG and MRI data has been highlighted, demonstrating their relevance in personalized medicine and disease progression modeling, evaluation of metrics, including accuracy, sensitivity and specificity in the model's clinical applicability and predictive power are highly accountable (Gang Q [2024]).

Notwithstanding the earlier application of HHM, recent works by (Mielke N [2024])has shown that, existing evidence suggests a link between ABO blood type and severe outcomes in coronavirus disease 2019 (COVID-19), hence assessing the relationship between blood type and severe outcomes across variant strains throughout the pandemic presents itself as a classical case for the application of HMM. In a recent study (Wei Zhang [2021]) utilizing Markov models is reporting that the expected duration of stay for patients infected with COVID-19 is approximately 14 days. Significant differences were observed between patient groups in terms of complications, with factors such as gender, age, hypertension, coronary heart disease, shortness of breath, myocardial damage, and thrombocytopenia showing statistically significant variations. Additionally, logistic multivariate regression analyses are identifying key clinical risk factors for COVID-19 patients. These factors primarily include gender, age, and the presence of comorbidities such as hypertension, coronary heart disease, shortness of breath, myocardial damage, and thrombocytopenia.

Moreover, another study (Soper BC [2022]) investigating the disease state-dependent risk profiles of patient demographics and medical comorbidities asso-

ciated with adverse outcomes of severe acute respiratory syndrome coronavirus 2 (SARS-CoV-2) infections. A covariate-dependent, continuous-time hidden Markov model with four states (moderate, severe, discharged, and deceased) is being utilized to model the dynamic progression of COVID-19 during hospitalization. The findings are revealed that the association between patient-level covariates and the risk of progression is disease state-dependent. Notably, factors such as being male, being Black, or having a medical comorbidity are associated with an increased risk of progressing from the moderate to the severe disease state. However, these same factors are correlating with a decreased risk of transitioning from the severe disease state to the deceased state.

2.2 Bayesian Hidden Markov Models (BHMM)

Bayesian Hidden Markov Models (BHMMs) build on the standard HMC framework, including Bayesian inference methods for model estimation and parameter learning. BHMMs have received a lot of interest because of their capacity to manage uncertainty, integrate previous information, and give principled approaches for model selection. The paper of Beal M. J. [2002] presented the Bayesian framework for training HMMs, which significantly impacted the development of BHMMs. Beal and colleagues solved the overfitting problems and model complexity inherent in standard maximum likelihood estimate techniques by using Bayesian inference. Their study highlighted the benefits of Bayesian approaches for capturing uncertainty and giving strong estimates, even in settings with little data. In recent years (Rojas-Salazar et al. [2020] Shaochuan [2019] Murakami [2009]), BHMMs have found applications in a variety of domains. For example, Ghahramani Z. [1997] suggested a variational Bayesian strategy for learning BHMMs and used it to the problem of voice recognition, attaining comparable performance to standard approaches. Despite the computing limitations of Bayesian inference, BHMMs remain an active field of study, with continuous efforts aimed at creating efficient algorithms, scalable methodologies, and real-world applications. One frequent use of BPMC is to model count data, in which the number of occurrences of an event is represented by a Poisson distribution using Bayesian inference for parameter estimate. By adding previous knowledge into the modeling process, BPMC may provide more accurate estimates and better reflect uncertainty in parameter estimations. . In the natural language processing sector, Tran T. [2016] suggested a Bayesian non-parametric strategy for modeling sequential data using Dirichlet process-based BHMMs. Their findings revealed the effectiveness of Bayesian nonparametrics in automatically establishing the right model complexity and capturing the underlying structure of sequential data. In computational biology, Liao Y. [2018] proposed a Bayesian hierarchical strategy for interpreting single-cell RNA sequencing data using BHMMs. Their findings demonstrated the

efficacy of BHMMs in simulating the variability seen in single-cell gene expression patterns and recognizing various cell types. In time-series analysis, Fox E. B. [2015] created a Bayesian framework for inferring latent states and dynamics in complex systems using BHMMs. Their findings demonstrated the effectiveness of BHMMs in detecting hidden patterns and dynamics in noisy observational data.

3 Methodology

3.1 BP-HMM to ABO blood type distribution

Suppose

$$N_c^{O^+} = (n_1^{O^+}, n_2^{O^+}, \ldots, n_m^{O^+}, N_c^{A^+} = (n_1^{A^+}, n_2^{A^+}, \ldots, n_m^{A^+}), \ldots, N_c^{AB^+} \tag{1}$$

$$= (n_1^{AB^+}, n_2^{AB^+}, \ldots, n_m^{AB^+}) \tag{2}$$

are counts of number of cases of COVID-19 for blood types, while $O^+, A^+, \ldots, AB^-$ while $c = 1, 2, \ldots, m$ specify a particular country with COVID-19 infection cases. This can be simplified in contingency table form as in Table 1

Table 1: Description of COVID-19 cases per blood type are distributed

Country(c)	O^+	A^+	B^+	AB^+	O^-	A^-	B^-	AB^-	Total
1	$n_1^{O^+}$	$n_1^{A^+}$	.	.	.	.	.	$n_1^{AB^-}$	N_1
2	$n_2^{O^+}$	$n_2^{A^+}$	.	.	.	.	.	$n_2^{AB^-}$	N_2
.	.	.	.	.	.	.	.	.	.
.	.	.	.	.	.	.	.	.	.
.	.	.	.	.	.	.	.	.	.
m	$n_m^{O^+}$	$n_m^{A^+}$	.	.	.	.	.	$n_m^{AB^-}$	N_c
Total	$N_{mc}^{O^+}$	$N_{mc}^{A^+}$	.	.	.	.	.	$N_{mc}^{AB^+}$	N

Assuming the number of cases for each blood type $N_c^{O^+}, N_c^{A^+}, \ldots, N_c^{AB^-}$ is governed by an unobserved(latent) process, $Y_c^{O^+} = \{y_1^{O^+}, y_2^{O^+}, \ldots, y_m^{O^+}\}, Y_c^{A^+} = \{y_1^{A^+}, y_2^{A^+}, \ldots, y_m^{A^+}\}, \ldots, Y_c^{AB^-} = (y_1^{AB^-}, y_2^{AB^-}, \ldots, y_m^{AB^-})$ respectively. Further, assume the number of cases is independent. Then the model for each of the number of cases $\{N_c^{O^+}, N_c^{A^+}, \ldots, N_c^{AB^-}\}$ is assumed Poisson distribution with mean, $\theta_E^{O^+} = \{\theta_1^{O^+}, \theta_2^{O^+}, \ldots, \theta_K^{O^+}\}, \theta_E^{A^+} = \{\theta_1^{A^+}, \theta_2^{A^+}, \ldots, \theta_K^{A^+}\}, \ldots, \theta_E^{AB^-} = \{\theta_1^{AB^-}, \theta_2^{AB^-}, \ldots, \theta_K^{AB^+}\}$ on a finite state space

$E = (1, \ldots, K)$ i.e.,

$$\omega(N_c^{O^+}|Y_c^{O^+}) = \text{E} \sim \text{Poisson}(\theta_K^{O^+}) \tag{3}$$

$$\omega(N_c^{A^+}|Y_c^{A^+}) = \text{E} \sim \text{Poisson}(\theta_K^{A^+}) \tag{4}$$

$$\vdots$$

$$\omega(N_c^{AB^-}|Y_c^{AB^-}) = \text{E} \sim \text{Poisson}(\theta_K^{AB^-}) \tag{5}$$

Meaning the number of COVID-19 infection count for each blood type $\{N_c^{O^+}, N_c^{A^+}, \ldots, N_c^{AB^-}\}$ depends on unobserved $\{Y_c^{O^+}, Y_c^{A^+}, \ldots, Y_c^{AB^-}\}$ process where $\{\theta_E^{O^+}, \theta_E^{A^+}, \ldots, \theta_E^{AB^-}\}_{E=(1,\ldots,K)}$ are state-dependent means of COVID-19 cases for each blood type in the finite state space.

Therefore, assuming a Poisson-Hidden Markov Model $\{N_c^{O^+}, N_c^{A^+}, \ldots, N_c^{AB^-}\}$ on a finite state space $E = (1, \ldots, K)$, where the unobserved (latent) $\{Y_c^{O^+}, Y_c^{A^+}, \ldots, Y_c^{AB^-}\}$ processes is the Markov Chain with Transition Probability for each blood types denoted by $\{P^{O^+}, P^{A^+}, \ldots, P^{AB^-}\}$. The initial state is assumed to have a uniform distribution on $E = (1, \ldots, K)$ which is the least informative choice and with a large number of iterations, the choice of the prior on the initial state has less influence on the inference.

In Bayesian structure the transition probabilities, $\{P_i^{O^+}, P_i^{A^+}, \ldots, P_i^{AB^-}\}$ and each mean of COVID-19 infection cases $\theta_i^{O^+}, \theta_i^{A^+}, \ldots, \theta_i^{AB^-}, i = (1, \ldots, K)$ are all unknown parameters. In the transition probability matrix component, it is assumed that each, $P_i^{O^+} = \{P_{i1}^{O^+}, P_{i2}^{O^+}, \ldots, P_{iK}^{O^+}\}, P_i^{A^+} = \{P_{i1}^{A^+}, P_{i2}^{A^+}, \ldots, P_{iK}^{A^+}\}$, $\ldots, P_i^{AB^-} = \{P_{i1}^{AB^-}, P_{i2}^{AB^-}, \ldots, P_{iK}^{AB^-}\}$, i.e., the i^{th} row of each transition probability follows a Dirichlet distribution, $P_i^{O^+} \sim \text{Dir}(\mu_{i1}^{O^+}, \mu_{i2}^{O^+}, \ldots, \mu_{iK}^{O^+}), P_i^{A^+} \sim \text{Dir}(\mu_{i1}^{A^+}, \mu_{i2}^{A^+}, \ldots, \mu_{iK}^{A^+}), \ldots, P_i^{AB^-} \sim \text{Dir}(\mu_{i1}^{AB^-}, \mu_{i2}^{AB^-}, \ldots, \mu_{iK}^{AB^-})$ which can be expressed in probability density function as:

$$\omega(P_i^{O^+}) \sim \prod_{j=1}^{K} P_{ij}^{(O^+)\mu_{ij-1}} \tag{6}$$

$$\omega(P_i^{A^+}) \sim \prod_{j=1}^{K} P_{ij}^{(A^+)\mu_{ij-1}} \tag{7}$$

$$\vdots$$

$$\omega(P_i^{AB^-}) \sim \prod_{j=1}^{K} P_{ij}^{(AB^-)\mu_{ij-1}} \tag{8}$$

Where μ_{ij} is the parameter vector and $i, j = 1, \ldots, K$. This implies $P_i's$ are here independent of each other. Where $\mu ij \geq 0$ and $P_{ij} \geq 0$ and $\sum P_{ij} = 1$ Assuming

Gamma prior for each of the state-dependent means $\{\theta_i^{O^+}, \theta_i^{A^+}, \ldots, \theta_i^{AB^-}\}$ for a given state $i = (1, \ldots, K)$. i.e.,

$$\theta_i^{O^+} \sim \gamma(\alpha_i^{O^+}, \beta_i^{O^+}) \tag{9}$$

$$\theta_i^{A^+} \sim \gamma(\alpha_i^{A^+}, \beta_i^{A^+}) \tag{10}$$

$$\vdots$$

$$\theta_i^{AB^+} \sim \gamma(\alpha_i^{AB^+}, \beta_i^{AB^+}) \tag{11}$$

Here, $\theta_i^{O^+}, \theta_i^{A^+}, \ldots, \theta_i^{AB^-}$ are independent of each other. The independence of prior distribution is a result of no association of information between states. Therefore, given number of COVID-19 cases by each country according to their blood type distributions as: $N_c^{O^+} = (n_1^{O^+}, n_2^{O^+}, \ldots, n_m^{O^+}), N_c^{A^+} = (n_1^{A^+}, n_2^{A^+}, \ldots,$ $n_m^{A^+}), \ldots, N_c^{AB^+} = (n_1^{AB^+}, n_2^{AB^+}, \ldots, n_m^{AB^+})$, we are interested in the joint posterior distribution of unknown parameters of each blood type $\pi^{O^+} =$ $(\theta_i^{O^+}, P_i^{O^+}), \ldots, \pi^{AB^-} = (\theta_i^{AB^-}, P_i^{AB^-})$. With the help of Gibbs sampler, we can draw samples from the joint posterior distribution since evaluating the joint posterior distribution of π computationally is not possible in close form.

Given the Markov chain, $(Y_j^{O^+}, Y_j^{A^+}, \ldots, Y_j^{AB^-})$ where, $j = 1, \ldots, K$ we estimate the full conditional distribution of the elements of $(P_i^{O^+}, P_j^{A^+}, \ldots, P_j^{AB^-})$ which is proportional to the prior probability distribution in equations 6 and its likelihood functions which is the multinomial distribution function as:

$$\begin{aligned} &\omega(P_i^{O^+}, P_j^{A^+}, \ldots, P_j^{AB^-} | Y_j^{O^+}, Y_{i,j}^{A^+}, \ldots, Y_{i,j}^{AB^-}) \propto \\ &\omega(P_j^{O^+}, P_j^{A^+}, \ldots, P_j^{AB^-}) \omega(Y_j^{O^+}, Y_j^{A^+}, \ldots, Y_j^{AB^-} | P_i^{O^+}, P_j^{A^+}, \ldots, P_j^{AB^-}) \end{aligned} \tag{12}$$

$$\begin{aligned} \omega(P_j^{O^+}) \omega(Y_j^{O^+} | P_j^{O^+}) &= \omega(P_j^{O^+} | \mu_{i,1}^{O^+}, \ldots, \mu_{i,j}^{O^+}) \prod_j^K \omega(Y_j^{O^+} | P_j^{O^-}) \\ &= \left(\frac{\prod_j^K \Gamma \mu_K}{\Gamma(\sum_j^K \mu_K)} \prod_{j=1}^K (P_j^{O+})^{\mu_{ij-1}} \right) \times \\ &\left(\frac{m!}{y_1^{O^+}! \ldots y_j^{O^+}!} (P_1^{O^+})^{y_1^{O^+}}, \ldots, P_j^{O^+})^{y_j^{O^+}} \right) \\ &\propto \prod_{j=1}^K (P_j^{O+})^{\mu_{ij-1}} \prod_{j=1}^K (P_j^{O+})^{\mathbf{1}\{y_c^{O^+}=j\}} \\ \omega(P_j^{O^+} | Y_j^{O^+}) &\propto \prod_{j=1}^K (P_j^{O+})^{\mu_{ij-1} + \sum \mathbf{1}\{y_c^{O^+}=j\}} \end{aligned} \tag{13}$$

Therefore, with the Gibb's sampler while given $(Y_j^{O^+}, Y_j^{A^+}, \ldots, Y_j^{AB^-})$ the full conditional distribution of each of $P_j^{O^+}, P_j^{A^+}, \ldots, P_j^{AB^-}$ is derived as

$$\omega(P_j^{O^+}|Y_j^{O^+}) \sim \text{Dirichlet}\left(\mu_{ij}^{O^+} + \sum \mathbf{1}\{Y_c^{O^+} = j\}\right) \tag{14}$$

$$\omega(P_j^{A^+}|Y_j^{A^+}) \sim \text{Dirichlet}\left(\mu_{ij}^{A^+} + \sum \mathbf{1}\{Y_c^{A^+} = j\}\right) \tag{15}$$

$$\vdots$$

$$\omega(P_j^{AB^-}|Y_j^{AB^-}) \sim \text{Dirichlet}\left(\mu_{ij}^{AB^-} + \sum \mathbf{1}\{Y_c^{AB^-} = j\}; i, j = (1, 2, \ldots, K)\right) \tag{16}$$

Where each of $\sum \mathbf{1}\{Y_c^{'} = j\}$ is an indicator function that represents the counts of instances $\{Y_c^{'} = j\}$ in the simulated sample path of the Markov chain. Here, the $P_j^{'}s$ are also obtained as independent Dirichlet vectors.

Next is the derivation of the posterior distribution $(\theta_j^{O^+}, \theta_j^{A^+}, \ldots, \theta_j^{AB^-})$ which has Gamma prior with Poisson distribution function as its likelihood. Given the State-dependent means $\theta_i^{O^+}, \theta_i^{A^+}, \ldots, \theta_i^{AB^-}$ and the Transition Probability $(P_i^{O^+}, P_i^{A^+}, \ldots, P_i^{AB^-})$ the joint likelihood function for the observations and the Markov-Chain is given as:

$$\begin{aligned}\omega(N_c^{O^+}, Y_j^{O^+}|\theta_i^{O^+}, P_i^{O^+}) &= \omega(n_1^{O^+}|y_1^{O^+}, \theta_1^{O^+}), \ldots, \omega(n_m^{O^+}|y_m^{O^+}, \theta_K^{O^+}) \\ &\quad \times \omega(y_1^{O^+}|P_1^{O^+}, \ldots, y_m^{O^+}|P_k^{O^+})\end{aligned} \tag{17}$$

$$\omega(N_c^{O^+}|Y_j^{O^+}\theta_i^{O^+}, P_i^{O^+}) = \prod_{i=1}^{K}\left\{\prod_{c=1}^{m} P_{y_{c,y_{c+1}}}^{O^+} \frac{\left(\theta_i^{O^+}\right)^{n_c^{O^+}}}{n_c^{O^+}!} e^{-\theta_i^{O^+}}\right\}$$

$$\omega(N_c^{O^+}|Y_j^{O^+}\theta_i^{O^+}, P_i^{O^+}) = \prod_{i=1}^{K}\left\{[\theta_i^{O^+}]^{\sum_c^m \mathbf{1}(Y_c^{O^+}=\mathbf{i})n_c^{O^+}} e^{-\theta_i^{O^+}\cdot\sum_c^m \mathbf{1}(Y_c^{O^+}=\mathbf{i})}\right\} \tag{18}$$

Next, we derive the posterior distribution which has Gamma prior from equation (3.38-3.40) with its likelihood function in equation (3.47) as

$$\omega(\theta_j^{O^+}|N_c^{O^+}, Y_j^{O^+}, \theta_j^{O^+}) = \theta_j^{O^+} \sim \gamma(\alpha_j^{O^+}, \beta_j^{O^+}) \times \omega(N_c^{O^+}|Y_j^{O^+}, \theta_j^{O^+}, P_j^{O^+}) \tag{19}$$

$$\omega(\theta_j^{O^+}|N_c^{O^+}, Y_j^{O^+}, \theta_j^{O^+}) \propto$$

$$\prod_j^k [\theta_i^{O^+}]^{\alpha_j^{O^+}-1} e^{-\beta_j^{O^+}\theta_j^{O^+}} \times \prod_{j=1}^{K}\left\{[\theta_j^{O^+}]^{\sum_c^m \mathbf{1}(Y_c^{O^+}=\mathbf{j})n_c^{O^+}} e^{-\theta_j^{O^+}\cdot\sum_c^m \mathbf{1}(Y_c^{O^+}=\mathbf{j})}\right\} \tag{20}$$

$$\omega(\theta_j^{O^+}|N_c^{O^+}, Y_j^{O^+}, \theta_j^{O^+}) \propto$$

$$\prod_{j=1}^{K}\left\{[\theta_j^{O^+}]^{\alpha_j^{O^+}-1+(\sum_c^m \mathbf{1}(Y_c^{O^+}=\mathbf{j})n_{jc}^{O^+})} \times e^{-\beta_j^{O^+}\theta_j^{O^+}+(-\theta_i^{O^+}\cdot\sum_c^m \mathbf{1}(Y_c^{O^+}=\mathbf{j}))}\right\} \tag{21}$$

$$\omega(\theta_j^{O^+}|N_c^{O^+}, Y_j^{O^+}, \theta_j^{O^+}) \propto$$

$$\prod_{j=1}^{K}\left\{[\theta_j^{O^+}]^{\alpha_j^{O^+}-1+\sum_c^m \mathbf{1}(Y_c^{O^+}=\mathbf{j})n_{jc}^{O^+}} e^{-\theta_j^{O^+}(\beta_j^{O^+}+\sum_c^m \mathbf{1}(Y_c^{O^+}=\mathbf{j}))}\right\} \tag{22}$$

The full conditional posterior distribution of the mean of each blood type, $\theta_j^{O^+}, \theta_j^{A^+}, \ldots, \theta_j^{AB^-}$ is obtained as

$$\theta_j^{O^+}|N_c^{O^+}, Y_j^{O^+} \sim \gamma\left(\alpha_j^{O^+}-1+\sum_c^m \mathbf{1}(Y_c^{O^+}=\mathbf{j})n_{jc}^{O^+}, \quad \beta_j^{O^+}+\sum_c^m \mathbf{1}(Y_c^{O^+}=\mathbf{j})\right) \tag{23}$$

(24)

$$\theta_j^{A^+}|N_c^{A^+}, Y_j^{A^+} \sim \gamma\left(\alpha_j^{A^+}-1+\sum_c^m \mathbf{1}(Y_c^{A^+}=\mathbf{j})n_{jc}^{A^+}, \quad \beta_j^{A^+}+\sum_c^m \mathbf{1}(Y_c^{A^+}=\mathbf{j})\right) \tag{25}$$

$$\vdots$$

$$\theta_j^{AB^-}|N_c^{AB^-}, Y_j^{AB^-} \tag{26}$$

$$\sim \gamma\left(\alpha_j^{AB^-}-1+\sum_c^m \mathbf{1}(Y_c^{AB^-}=\mathbf{j})n_{jc}^{AB^-}, \quad \beta_j^{AB^-}+\sum_c^m \mathbf{1}(Y_c^{AB^-}=\mathbf{j})\right)$$

$$; j=(1,2,\ldots,K)$$

Where, $\{\alpha_j^{O^+}, \alpha_j^{A^+}\ldots, \alpha_j^{AB^-}\}$ and $\{\beta_j^{O^+}, \beta_j^{A^+}\ldots, \beta_j^{AB^-}\}$ the prior shape and rate parameters for each blood type respectively. $\{\mathbf{1}(Y_c^{'}=j)\}$ is an indicator function representing each count of instances in the simulated sample path of the Markov chain. $\{\sum_{c=1}^n \mathbf{1}(Y_c^{'}=j)N_{jc}^{'}\}$ is the contribution of regime j to each of the observed values of $\{N_c^{O^+}, N_c^{A^+}, \ldots, N_c^{AB^-}\}$. In the Gibbs Sampler, the model will first generate a sample path of the Markov chain (MC). The model then uses this

sample path to decompose the observed counts into (simulated) regime contributions. Finally, with the availability of the Markov chain sample path, and the regime contributions, the developed model can now update $P_j^{O^+}, P_j^{A^+}, \ldots, P_j^{AB^-}$ and $\theta_j^{O^+}, \theta_j^{A^+} \ldots, \theta_j^{AB^-}$.

If the steps above are repeated for a large number of times, the resulting samples of values of $\hat{P}_j^{O^+}, \hat{P}_j^{A^+}, \ldots, \hat{P}_j^{AB^-}$ and $\hat{\theta}_j^{O^+}, \hat{\theta}_j^{A^+} \ldots, \hat{\theta}_j^{AB}$ provide the required estimates of their posterior distributions. In the posterior, the hidden states are ranked according to the state-dependent mean of infection occurrence respecting each blood type, i.e. $\hat{\theta}_j^{O^+} = \{\hat{\theta}_1^{O^+}, \hat{\theta}_2^{O^+}, \ldots, \hat{\theta}_K^{O^+}\}, \theta_j^{A^+} = \{\hat{\theta}_1^{A^+}, \hat{\theta}_2^{A^+}, \ldots, \hat{\theta}_K^{A^+}\}, \ldots,$ $\hat{\theta}_j^{AB^-} = \{\theta_1^{AB^-}, \theta_2^{AB^-}, \ldots, \hat{\theta}_K^{AB^-}\}$ for a given state $j = 1, \ldots, K$. Given this, a smaller rate of infection occurring in a state is an indication of a lesser probability of getting that infection of that particular blood type.

The deviance information criterion (DIC) is used as a measure of model comparison and adequacy. Mathematically is given as $\mathrm{DIC}(K) = D(\hat{\theta}_K^{A^+}, K) + 2\tau$, where, is the deviance measure which is equal to minus twice the log-likelihood, is the posterior mean of the model for blood type and is the number of effective parameters for the model. Smaller DIC values indicate a better-fitting model.

In this study, using OpenBugs as a statistical tool, the Monte Carlo error, traceplot, and autocorrelations were monitored to check the convergence of the analyses. The Monte Carlo errors measure the variation of the mean of the parameter of interest due to the simulation. Therefore, a lower MC error in the comparison with the corresponding estimated posterior standard deviation is an indication that the posterior mean was estimated with high precision. The trace plot gives a plot of the generated values versus each iteration number. When there is an indication of no patterns or irregularities then we assumed convergence of the algorithm. The autocorrelation plots the chain of each parameter of interest. In this study, the plot was done using lag from 1 to 50 to monitor the autocorrelations. When a lower autocorrelation is observed for all parameters at a certain lag then that would imply that an independent sample can be obtained by re-running the algorithm with a *thin*-set equal to that lag as an update.

In the Bayesian paradigm, the choice of the prior distribution is driven by mathematical convenience rather than prior information [Zucchini et al., 2018].

4 Data Assimilation, Analysis and Results

The Bayesian Poisson Hidden Markov Model (BP-HMM) was used to analyze COVID-19 incidence counts by blood type distribution in sixteen (16) Ghanaian

areas. The study data comes from the Ghana Health Service's COVID-19 dashboard as of September 1st, 2021. These data sets were used in this study for two purposes: first, to determine whether the model would select the same hidden states for each blood type distribution across Ghana's sixteen (16) regions, and second, to compare the rate of infection across blood type distributions. This comparison is feasible since the research used the MCMC sampling technique, which includes 98,000 iterations and 2000 burn-ins.

For the avoidance of doubt For the avoidance of doubt, the blood types with hidden states are classified as shown in Table 2 with stage 1 being the severe condition stage and stage 5 being the early infection state. For a four-state transition hidden states, state 4 is the earliest of infection, with stage 1 being the detection stage of the transmission.

Table 2: Hidden States of Blood Type COVID-19 Infections

	5 States	4 States
State 1	Catastrophe	Detected
State 2	Detected	Symptomatic
State 3	Symptomatic	Asymptomatic
State 4	Asymptomatic	Healthy
State 5	Healthy	

4.1 Selection of Hidden States Associated with the Blood Type Distribution in COVID-19 Patients in Ghana

The Deviance Information Criterion (DIC) is used to determine how many concealed states are present. The figures show the lower DIC for each blood type distribution within a certain number of states, as well as the connected states. Table 3 provides a crucial model comparison for model selection. In the table, τ represents the number of parameters, whereas i represents the number of hidden states. For BP-HMM, $i = \tau^2$. In this scenario, the model evaluates the lower DIC and selects the optimal choice. Table 3 shows that blood types $O^+, O^-, A^+, A^-, B^+, B^-, AB^+$ selected five [5] states for the Ghana COVID-19 datasets, whereas blood type AB^- picked four [4]. Consistent hidden states of five (5) were found for seven blood and rhesus types, with only blood mixed with the rhesus factor having a hidden state of four.

Table 3: Summary results of model selection for COVID-19 cases of blood type

Blood Type	(BP-HMM) Selected State (K)	τ	Deviance	DIC
O^+	5	25	1541.58	1591.58
A^+	5	25	584.6	634.6
B^+	5	25	603.58	653.58
AB^+	5	25	176.44	226.44
O^-	5	25	226.61	276.61
A^-	5	25	126.13	176.13
B^-	5	25	124.53	174.53
AB^-	4	16	79.24	129.24

4.2 Estimated Average Transition Probabilities and Convergence

The estimated posterior mean for the different blood type distributions is correct since the MC error relative to each associated estimated posterior standard deviation (MC error%) is small in all cases. Tables 4 to 7 show that for a sample of 98000 iterations after deleting 2000 as a burin, each MC error is smaller than the corresponding standard deviation provided a lower MC error% in the range 0.2971% - 1.5236%. The approach is assumed to be convergent since there are no patterns or abnormalities in trace plot data (Figure 1). The posterior summaries provide detailed insights into the distribution of blood types, highlighting significant variations in prevalence and precision across groups. Blood type O^+ demonstrates the highest mean distribution, indicating its predominance in the studied population, while O^-, A^-, B^-, and AB^- exhibit lower means, reflecting their rarity and critical importance in medical emergencies. Blood types A^+ and B^+ show moderately high mean values, aligning with global trends of their commonality. In contrast, AB^+ and AB^- are the least represented, underscoring the need for targeted donor recruitment and resource planning. The low Monte Carlo (MC) error percentages across all groups validate the robustness of the Bayesian model, ensuring reliable estimates for healthcare planning, policy formulation, and epidemiological studies.

Table 4: Posterior summary of the estimated mean for blood type O^+

	Mean	SD	MC error	MC error%	Val2.5%	Median	Val97.5%	start	sample
				O^+					
[1]	334	7.438	0.0287	0.3858	319.5	348.7	348.7	2001	98000
[2]	1005.1	15.76	0.069	0.4378	974.6	1005	1037	2001	98000
[3]	2878.4	26.77	0.0996	0.372	2826	2879	2931	2001	98000
[4]	10774.5	103.9	0.4616	0.4442	10570	10770	10980	2001	98000
[5]	31968.4	173.4	0.5628	0.3245	31630	31970	32310	2001	98000
				O^-					
[1]	27.1	3.136	0.0463	1.4764	18.8	27.54	32.27	2001	98000
[2]	83	5.919	0.0804	1.3583	69.39	83.58	93.42	2001	98000
[3]	241.2	7.737	0.0279	0.3606	226.3	241.1	256.6	2001	98000
[4]	901.8	29.97	0.119	0.397	843.7	901.6	961.4	2001	98000
[5]	2674.1	49.73	0.1601	0.3219	2578	2674	2772	2001	98000

4.3 Hidden -States Infection Rates with COVID-19 Infection Stages (Number of Hidden States)

The study reveals that the incidence of infection is directly linked to the number of states, as shown in Table 8. This means that as the number of states increases for each blood type, the infection rate also rises, leading to a higher estimated number of infected individuals. Specifically, blood type O^+ has the highest total estimated infections (approximately 46,961), while blood types AB^- has the lowest (around 261). In general, the estimated infection rates follow a pattern where more common blood types like O^+, B^+, and A^+ have higher infection numbers, whereas rarer types like AB^- have fewer. This suggests that the spread of infection increases with the number of states, which could imply the importance of broader surveillance and control measures across multiple regions.

Table 9 displays the estimated percentage rate of infection per state for blood types and associated rhesus factors among Ghana COVID-19 participants. The results demonstrate that in state [1], the infection rate differs by blood type, with positive rhesus factors infected more often than negative rhesus factors. Except for blood type AB+, the infection rate for positive rhesus factors in the state [1]

Table 5: Posterior summary of the estimated mean for blood type A^+

	Mean	SD	MC error	MC error%	Val2.5%	Median	Val97.5%	start	sample
				A^+					
[1]	109.3	4.28	0.017	0.3971	101.1	109.3	117.8	2001	98000
[2]	328.7	9.085	0.0358	0.394	311.3	328.6	346.9	2001	98000
[3]	942.3	15.4	0.0551	0.3577	912.6	942.2	972.7	2001	98000
[4]	3525.5	59.5	0.2609	0.4384	3410	3525	3642	2001	98000
[5]	10458.6	98.5	0.2969	0.3014	10270	10460	106550	2001	98000
				A^-					
[1]	8.14	1.714	0.0184	1.0735	4.544	8.207	11.45	2001	98000
[2]	25.3	3.32	0.0342	1.0301	19.36	25.23	32.15	2001	98000
[3]	75.28	4.37	0.0147	0.3363	66.96	75.16	84.08	2001	98000
[4]	281.03	16.77	0.0677	0.4036	249.1	280.8	314.8	2001	98000
[5]	832.4	27.82	0.0851	0.3058	779	832	887.9	2001	98000

seems to be around 0.7. Insights across the states show that a substantially larger proportion of rates happened in state [5], followed by state [4]. This trend appears to be accepted due to the transition requirements from one state to another, with state [5] being an early stage of infection and state [1] being the worst state of infection. Thus, more infected individuals are expected to be within the early stages of infection, with few individuals being in the compartment of worse case stages due to the low fatality recorded in Ghana for COVID-19. Table 10 shows that state transition percentages are highest in the early stages for all blood types and lowest in the worst stage. However, blood types with a positive rhesus factor had a higher risk of developing a severe COVID-19 infection.

4.4 Analysis of Hidden Markov Chain for Blood Types

In this section, Hidden Markov Chains (HMMs), as a valuable tool for modeling systems with hidden states whose behavior can only be deduced from observable outcomes, are presented. This is a critical step in understanding the dynamics of complex systems and extracting relevant insights. In this section, the study looks at the estimate of transition probabilities inside the hidden Markov model, which is an important feature that offers insight into the underlying structure and development of COVID-19 infection graduating states within the blood types and corresponding rhesus factors. The goal is to uncover the complicated linkages between hidden states that can only be detected via seen data sequences. By methodically predicting the transition probabilities between these latent states, we hope to discover and understand patterns, trends, and dependencies that regulate the stages of the infection amid the blood types.

Table 6: Posterior summary of the estimated mean for blood type B^+

	Mean	SD	MC error	MC error%	Val2.5%	Median	Val97.5%	start	sample
				B^+					
[1]	113.7	4.371	0.0179	0.4095	105.4	113.8	122.6	2001	98000
[2]	342.2	9.289	0.0404	0.4349	324.2	342.2	360.7	2001	98000
[3]	979.4	15.68	0.0518	0.3303	949.3	979.6	1010	2001	98000
[4]	3665.9	60.83	0.2488	0.409	3548	3666	3786	2001	98000
[5]	10875.4	100.7	0.2992	0.2971	10680	10870	11070	2001	98000
				B^-					
[1]	7.29	1.782	0.0225	1.2626	3.359	7.412	10.58	2001	98000
[2]	23.33	3.238	0.0375	1.1581	17.52	23.22	29.89	2001	98000
[3]	70.01	4.19	0.0148	0.3532	62.05	69.94	78.45	2001	98000
[4]	260.9	16.06	0.0674	0.4196	230.6	260.7	293.6	2001	98000
[5]	773.1	26.68	0.0901	0.3377	721.8	772.9	826.2	2001	98000

Table 7: Posterior summary of the estimated mean for blood type AB^+

	Mean	SD	MC error	MC error%	Val2.5%	Median	Val97.5%	start	sample
				AB^+					
[1]	15.5	3.019	0.046	1.5236	9.352	15.97	20.56	2001	98000
[2]	49.26	5.063	0.07	1.3825	40.06	49.27	58.92	2001	98000
[3]	149.9	6.121	0.02	0.3267	138.3	149.9	162.2	2001	98000
[4]	562	23.76	0.097	0.4082	516.4	561.8	609.9	2001	98000
[5]	1664.7	39.3	0.12	0.3053	1589	1589	1742	2001	98000
				AB^-					
[1]	3.73	0.651	0.001	0.1536	3.293	3.293	5.099	2001	98000
[2]	16.09	2.217	0.013	0.5863	14.57	16.03	20.61	2001	98000
[3]	62.02	7.856	0.041	0.5218	56.54	61.72	78.38	2001	98000
[4]	179.59	12.88	0.09	0.6987	170.7	179.3	188.1	2001	98000

4.4.1 Analysis of the Blood Type O^+ and O^-

The Hidden Markov Chain (HMC) analysis reveals significant differences in the infection progression and recovery probabilities between individuals with blood types O^+ and O^-. By examining the transition probabilities between infection states, the findings offer key insights into how blood type may influence disease outcomes.

For individuals with the O^+ blood type, the transition from severe infection states to milder ones is notably higher. The transition probability from state $[5, 1]$ (most severe phase) to state $[1, 1]$ (least severe phase) is 0.3634, the highest among all transitions for O^+ individuals (Table 11). This suggests that individuals with this blood type are more likely to recover from the most severe stages of infection. Additionally, the transition probabilities from state $[1, 2]$ (mild to moderate)

Table 8: Summary Statistic of Blood Types by States for Ghana (GH)

Blood Type	State [1]	State [2]	State [3]	State [4]	State [5]	Total
$\hat{\theta}_i^{GH-O^+}$	334.08	1005.18	2878.40	10774.59	31968.48	46,960.73
$\hat{\theta}_i^{GH-O^-}$	27.15	83.00	241.28	901.83	2674.17	3927.43
$\hat{\theta}_i^{GH-A^+}$	109.32	328.75	942.30	3,525.52	10,458.68	15,364.57
$\hat{\theta}_i^{AF-A^-}$	8.14	25.30	75.28	281.03	832.43	1222.18
$\hat{\theta}_i^{GH-B^+}$	113.77	342.28	979.48	3,665.93	10,875.47	15,976.93
$\hat{\theta}_i^{GH-B^-}$	7.29	23.33	70.01	260.95	773.19	1134.77
$\hat{\theta}_i^{GH-AB^+}$	15.50	49.26	149.99	562.01	1664.76	2441.52
$\hat{\theta}_i^{GH-AB^-}$	3.73	16.09	62.02	179.59	-	261.43

Table 9: Estimated percentage rate of infection per state of blood types and Rhesus for Ghana COVID-19

Blood Type	State [1]	State [2]	State [3]	State [4]	State [5]
O+	0.71	2.15	6.13	22.94	68.07
O-	0.69	2.11	6.14	22.96	68.08
A+	0.71	2.13	6.14	22.95	68.08
A-	0.66	2.07	6.2	23	68.07
B+	0.71	2.14	6.13	22.94	68.06
B-	0.64	2.05	6.17	22.99	68.13
AB+	0.63	2.01	6.14	23.01	68.21

Table 10: Estimated percentage rate of infection per state of blood types for Ghana COVID-19

Blood Type	State [1]	State [2]	State [3]	State [4]	State [5]
O	0.7	2.13	6.14	22.95	68.07
A	0.68	2.1	6.17	22.98	68.07
B	0.67	2.1	6.15	22.97	68.17
AB	0.32	4.08	14.93	46.57	34.11

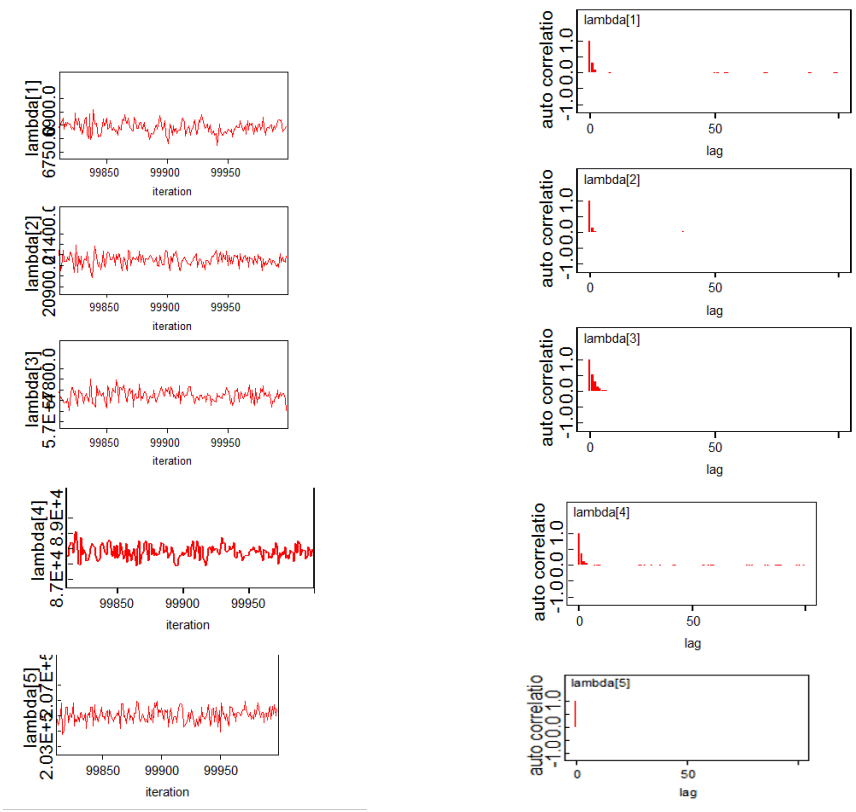

Figure 1: Patterns and Anomalies

and state $[4, 2]$ (severe to moderate) are also significant, with values of 0.3272 and 0.3313, respectively. These findings suggest a higher likelihood of recovery and stabilization for O^+ individuals compared to other blood types. The higher transition probabilities from severe to milder states indicate that individuals with blood type O^+ may have a more favorable prognosis in terms of recovery. This suggests that O^+ individuals are less likely to experience a worsening of their condition and may require less intensive medical intervention during the course of the infection (Table 11). In contrast, individuals with blood type O^- appear to face a more challenging course of infection. The transition probability from state $[1, 1]$ (severe) to the same state, 0.5132, is the highest among all transitions for O^- individuals (Table 12). This suggests that O^- individuals are more likely to remain in severe stages of infection and are less likely to progress to milder states. Further, the transition probabilities from state $[1, 2]$ (mild to moderate) and state $[2, 1]$ (moderate to mild) are comparatively low at 0.1634 and 0.1568, respectively, indicating a reduced likelihood of improvement for O^- individuals once they have reached a severe phase (Table 12). The findings imply that individuals

with blood type O^- may have a higher risk of prolonged illness or deterioration, which could warrant more intensive monitoring and medical care. Their lower transition probabilities to less severe states suggest that early intervention may be critical to prevent further complications. These results underscore the potential role of blood type in influencing the course of infectious diseases. For blood type O^+ individuals, the higher transition probabilities from severe to milder infection stages indicate a greater likelihood of recovery, which could inform more lenient management strategies for this group. On the other hand, individuals with blood type O^- face a higher risk of remaining in or deteriorating into severe stages of infection. This suggests the need for targeted and possibly more aggressive treatment and monitoring for O^- individuals.

4.4.2 Analysis of the Blood Type A^+ and A^-

Blood groups A^+ and A^- type did not see worse transitions comparatively to the O^- blood group type. As shown in Table 13 and Table 14, transitions from state 1 and state 2 to other states were all lower than 0.3, except in the state [1,2] in the A^- which recorded a transition probability of 0.3764, however since the transition is from state 1 to state 2, such a high probability of transition is for improvement of health condition, and positive results for the management of the infection.

For individuals with the A^+ blood type, the transition probabilities generally indicate stable health states across the five defined health states. The most notable transition occurs from state 1 (initial state) to state 2, with a probability of 0.3961. This suggests that individuals with A^+ blood type are relatively more likely to improve or recover during the infection period. Importantly, the probabilities of transitioning to more negative health states (such as state 3, state 4, and state 5) are lower, reflecting the possibility that individuals with A^+ blood type may be more resilient to deterioration. Overall, the distribution of transition probabilities for the A^+ group suggests a trend towards health stability, with positive outcomes being more probable than negative ones. The relatively lower transition probabilities to worse health states indicate that this group may have better baseline resilience against infection and related health challenges. In conclusion, individuals with A^+ blood type tend to experience fewer dramatic fluctuations in their health status and are more likely to show improvement with treatment. Individuals with A^- blood type exhibit a higher probability of transitioning from state 1 to state 2 (0.3764). This is a significant finding, as it suggests that individuals with A^- blood type are more likely to experience positive health outcomes and recovery during the infection period. However, the transition probabilities for other states are more scattered, particularly for the negative health states (states 4 and 5), indicating a

greater range of health outcomes for this group. The higher variability in transitions, coupled with the relatively high transition probability to state 2, suggests that individuals with A^- blood type may show a broader spectrum of responses to infection and management interventions. While some may experience recovery, others could face deterioration in health. This variability may indicate that people with A^- blood type could benefit from more tailored or personalized treatment strategies to address the different health outcomes they may experience.

Table 11: Estimated Posterior Hidden Transition Probability for Ghana Blood Type O^+

GH O+	Average	StanDev	MC_error	2.5Percent	Median	97.5 Percent
State[1,1]	0.2429	0.1414	0.004653	0.03439	0.2211	0.5619
State[1,2]	0.3272	0.1478	0.004288	0.08465	0.3128	0.64
State[1,3]	0.1071	0.09678	0.00265	0.002887	0.07928	0.3607
State[1,4]	0.2115	0.1285	0.003486	0.0307	0.1899	0.5147
State[1,5]	0.1112	0.1012	0.002989	0.002996	0.08189	0.375
State[2,1]	0.2801	0.153	0.004797	0.04207	0.2595	0.6219
State[2,2]	0.2404	0.1376	0.003791	0.03409	0.2202	0.5579
State[2,3]	0.2388	0.1384	0.0041	0.03604	0.2169	0.5561
State[2,4]	0.121	0.1049	0.002867	0.003249	0.09169	0.3897
State[2,5]	0.1196	0.1076	0.003239	0.003466	0.09003	0.4024
State[3,1]	0.1603	0.1321	0.004053	0.005553	0.1284	0.4919
State[3,2]	0.1386	0.1202	0.002826	0.004254	0.106	0.4489
State[3,3]	0.2769	0.1545	0.005266	0.04239	0.2568	0.6163
State[3,4]	0.1402	0.1215	0.003276	0.004429	0.1071	0.4526
State[3,5]	0.284	0.1597	0.004911	0.04357	0.2617	0.6351
State[4,1]	0.1805	0.1475	0.003959	0.004709	0.1441	0.541
State[4,2]	0.3313	0.1796	0.00561	0.05042	0.3108	0.7151
State[4,3]	0.1603	0.1365	0.003443	0.004793	0.1246	0.5029
State[4,4]	0.1639	0.1383	0.004621	0.004647	0.1278	0.5112
State[4,5]	0.164	0.1383	0.00345	0.00553	0.1269	0.5141
State[5,1]	0.3634	0.1807	0.005465	0.06206	0.3501	0.7409
State[5,2]	0.1597	0.1335	0.003279	0.005148	0.1233	0.4948
State[5,3]	0.1579	0.1355	0.003856	0.004864	0.122	0.5086
State[5,4]	0.1506	0.1339	0.003478	0.004257	0.1138	0.4962
State[5,5]	0.1684	0.1421	0.004532	0.005209	0.1318	0.5284

Table 12: Estimated Posterior Hidden Transition Probability for Ghana Blood Type O^-

GHO-	Average	StanDev	MC_error	2.5Percent	Median	97.5 Percent
State[1,1]	0.5132	0.1458	0.007044	0.2199	0.5195	0.7816
State[1,2]	0.1634	0.1107	0.004899	0.02131	0.1412	0.4356
State[1,3]	0.1531	0.1048	0.003619	0.0132	0.1315	0.4089
State[1,4]	0.08815	0.08149	0.003263	0.002587	0.06348	0.3012
State[1,5]	0.08217	0.0743	0.001991	0.002257	0.06134	0.2802
State[2,1]	0.1568	0.1307	0.003577	0.004847	0.1235	0.4811
State[2,2]	0.263	0.1445	0.00399	0.04195	0.2448	0.5785
State[2,3]	0.1492	0.1291	0.003443	0.004706	0.1132	0.4812
State[2,4]	0.1473	0.1255	0.003446	0.004695	0.114	0.4621
State[2,5]	0.2837	0.1641	0.005388	0.04043	0.2597	0.6475
State[3,1]	0.3376	0.1898	0.007315	0.03205	0.3212	0.7273
State[3,2]	0.1634	0.1418	0.003981	0.005102	0.1254	0.5246
State[3,3]	0.1682	0.1392	0.003911	0.005787	0.1313	0.509
State[3,4]	0.1657	0.1393	0.004025	0.005116	0.1299	0.5201
State[3,5]	0.1651	0.1427	0.004628	0.004414	0.1267	0.5265
State[4,1]	0.2413	0.1788	0.006502	0.009001	0.2048	0.6472
State[4,2]	0.1967	0.1647	0.005662	0.005673	0.1515	0.6059
State[4,3]	0.1949	0.1626	0.004479	0.005891	0.1515	0.5959
State[4,4]	0.1784	0.1491	0.00453	0.005618	0.1389	0.5544
State[4,5]	0.1887	0.1555	0.00391	0.005836	0.1511	0.571
State[5,1]	0.3518	0.1774	0.00511	0.06166	0.3358	0.7349
State[5,2]	0.155	0.1339	0.003921	0.004474	0.1167	0.4928
State[5,3]	0.1621	0.1395	0.003598	0.004791	0.1243	0.5176
State[5,4]	0.1633	0.1385	0.003834	0.004922	0.1263	0.5136
State[5,5]	0.1678	0.1359	0.003581	0.005245	0.1327	0.4962

4.4.3 Analysis of the Blood Type B^+ and B^-

Individuals with B^+ and B^- blood types have lower transition probabilities in state 5, indicating individuals with this blood group are unlikely to transition to other states. However, when it happens, state [5,1] indicates a transition probability of 0.3 to get worse; thus, once infected, their infection has a 30% chance of deteriorating into a worse form. Despite this, state [1,2] exhibited dominance transitions with a probability of 0.4009 for B^+ and 0.383 for B^-, suggesting that there are roughly 40.08 % and 38.9 % possibilities, respectively, to ameliorate the infection situation to gain a better or improved infection condition. The Hidden Markov Chain (HMC) model for blood types B^+ and B^- reveals important insights into disease progression. For both blood types, the probability of tran-

sitioning to state 5 is relatively low, indicating that once individuals reach this severe state, their likelihood of moving to other states decreases. This suggests a level of less stability but a prolong period of getting better, however, there remains a 0.30 probability of further deterioration into state [5,1], which highlights the risk of worsening conditions if not managed appropriately. Additionally, both blood types exhibit dominant transitions to state [1,2], with approximately 0.40 probability for B^+ and 0.38 for B^-. This suggests that, for the majority of individuals, improvement or stabilization is more likely than deterioration, pointing to a generally favorable prognosis.

Table 13: Estimated Posterior Hidden Transition Probability for Ghana Blood Type A^+

GHA+	Average	StanDev	MC_error	2.5Percent	Median	97.5 Percent
State[1,1]	0.2421	0.1394	0.003923	0.03546	0.223	0.5548
State[1,2]	0.3961	0.1624	0.005033	0.11	0.3879	0.7267
State[1,3]	0.1179	0.1041	0.00262	0.003391	0.08887	0.3907
State[1,4]	0.123	0.1082	0.003158	0.003873	0.0933	0.405
State[1,5]	0.121	0.1076	0.003119	0.003547	0.09116	0.3997
State[2,1]	0.2156	0.1265	0.003614	0.03408	0.1951	0.5077
State[2,2]	0.2417	0.1395	0.004422	0.03402	0.2194	0.5592
State[2,3]	0.2126	0.1279	0.003567	0.03021	0.1926	0.5073
State[2,4]	0.2174	0.1301	0.004471	0.02986	0.1973	0.5184
State[2,5]	0.1127	0.09658	0.002999	0.00337	0.08716	0.3593
State[3,1]	0.1464	0.1273	0.003588	0.00426	0.1115	0.4735
State[3,2]	0.152	0.1287	0.003275	0.004525	0.1197	0.4755
State[3,3]	0.2691	0.1491	0.004478	0.04114	0.2479	0.6022
State[3,4]	0.145	0.1264	0.003151	0.004001	0.1088	0.4696
State[3,5]	0.2875	0.1626	0.004286	0.04315	0.2646	0.6503
State[4,1]	0.1641	0.138	0.003616	0.00497	0.128	0.5127
State[4,2]	0.3579	0.1822	0.004922	0.06061	0.3412	0.7432
State[4,3]	0.1514	0.1313	0.003136	0.003841	0.1145	0.4865
State[4,4]	0.1679	0.1406	0.004054	0.005043	0.1314	0.5124
State[4,5]	0.1587	0.134	0.003192	0.005282	0.1236	0.4965
State[5,1]	0.3404	0.1809	0.005663	0.05331	0.3241	0.7265
State[5,2]	0.18	0.1487	0.004025	0.005845	0.1425	0.5555
State[5,3]	0.162	0.1392	0.003728	0.004607	0.1245	0.5116
State[5,4]	0.159	0.1358	0.003385	0.004683	0.121	0.5019
State[5,5]	0.1586	0.1323	0.004271	0.004981	0.1246	0.4946

Table 14: Estimated Posterior Hidden Transition Probability for Ghana Blood Type A^-

GHA-	Average	StanDev	MC_error	2.5Percent	Median	97.5 Percent
State[1,1]	0.2323	0.1457	0.004861	0.02087	0.2106	0.5627
State[1,2]	0.3764	0.1666	0.005638	0.09192	0.3649	0.7226
State[1,3]	0.118	0.1049	0.002824	0.003461	0.08834	0.3823
State[1,4]	0.1553	0.1252	0.003955	0.005026	0.1261	0.464
State[1,5]	0.118	0.1052	0.002584	0.003616	0.08832	0.3932
State[2,1]	0.2362	0.1401	0.00408	0.03474	0.2129	0.5585
State[2,2]	0.253	0.1442	0.004632	0.03833	0.2318	0.5768
State[2,3]	0.2172	0.1317	0.004216	0.03058	0.1954	0.5299
State[2,4]	0.1804	0.1295	0.004232	0.008837	0.1554	0.4921
State[2,5]	0.1131	0.103	0.003084	0.003112	0.08376	0.3801
State[3,1]	0.1478	0.1294	0.003525	0.004339	0.1125	0.4866
State[3,2]	0.1513	0.1269	0.003294	0.004653	0.1184	0.4703
State[3,3]	0.2804	0.1584	0.006055	0.04256	0.2549	0.6431
State[3,4]	0.1403	0.1253	0.003516	0.003791	0.1036	0.4585
State[3,5]	0.2802	0.1572	0.004279	0.03947	0.2602	0.6274
State[4,1]	0.1746	0.1426	0.00372	0.005311	0.1413	0.5373
State[4,2]	0.3483	0.1792	0.004871	0.05624	0.335	0.7222
State[4,3]	0.1652	0.1387	0.00353	0.004827	0.1292	0.5197
State[4,4]	0.1547	0.1274	0.003102	0.005019	0.1241	0.4707
State[4,5]	0.1571	0.1348	0.003533	0.004224	0.1205	0.502
State[5,1]	0.3415	0.1804	0.00537	0.05563	0.323	0.7253
State[5,2]	0.1781	0.1464	0.003883	0.006169	0.1403	0.5447
State[5,3]	0.1643	0.1382	0.003811	0.005612	0.1304	0.5145
State[5,4]	0.1631	0.1368	0.003856	0.005166	0.1283	0.5109
State[5,5]	0.153	0.1285	0.003557	0.004937	0.1195	0.4789

The findings imply that early intervention is key to capitalizing on these positive transitions, ensuring that individuals have a greater chance of recovery or stabilization rather than progressing to more severe states. The statistical uncertainty in the model is also noteworthy. For B^+, the probability of transitioning to state [1,2] is 0.4009 with a standard deviation of 0.1586, indicating variability in outcomes, with a confidence interval ranging from 0.1193 to 0.728. For B^-, the probability is 0.383, with a standard deviation of 0.1701, and a confidence interval of 0.08977 to 0.7314. This suggests that while improvement is likely for a significant portion of both groups, there is still some uncertainty in predicting individual outcomes. This result underscores the importance of timely medical in-

tervention to prevent deterioration, particularly in individuals who is yet to reach state 5, while also highlighting the relatively high probability of improvement for individuals with either blood type. Early clinical care can help mitigate risks and improve overall health outcomes, as a substantial proportion of individuals with B^+ and B^- blood types are likely to experience stabilization or recovery.

Table 15: Estimated Posterior Hidden Transition Probability for Ghana Blood Type B^+

GHB+	Average	StanDev	MC_error	2.5Percent	Median	97.5 Percent
State[1,1]	0.2378	0.1374	0.003875	0.03467	0.2184	0.551
State[1,2]	0.4009	0.1586	0.003824	0.1193	0.3947	0.728
State[1,3]	0.12	0.1065	0.002605	0.003502	0.08955	0.4016
State[1,4]	0.1194	0.107	0.003032	0.003397	0.08938	0.3949
State[1,5]	0.1219	0.1071	0.002821	0.00354	0.09208	0.3995
State[2,1]	0.2218	0.1314	0.004021	0.02913	0.2008	0.519
State[2,2]	0.2462	0.141	0.004249	0.03699	0.2266	0.5601
State[2,3]	0.2092	0.1296	0.004182	0.02862	0.1875	0.5229
State[2,4]	0.2158	0.1307	0.004113	0.03059	0.1933	0.5242
State[2,5]	0.107	0.09558	0.002577	0.002995	0.08008	0.3592
State[3,1]	0.1447	0.1252	0.003553	0.003974	0.1105	0.4654
State[3,2]	0.1592	0.1346	0.004235	0.00481	0.1233	0.5054
State[3,3]	0.2842	0.159	0.0053	0.04268	0.2615	0.6469
State[3,4]	0.1408	0.1229	0.003055	0.004068	0.107	0.4532
State[3,5]	0.2711	0.1582	0.005239	0.03591	0.2467	0.6273
State[4,1]	0.1597	0.1352	0.003625	0.004829	0.1227	0.506
State[4,2]	0.3517	0.181	0.004714	0.06179	0.3354	0.7292
State[4,3]	0.1663	0.1394	0.003653	0.004975	0.1285	0.5126
State[4,4]	0.1626	0.1366	0.004342	0.005057	0.1257	0.5113
State[4,5]	0.1598	0.1331	0.003219	0.005932	0.1263	0.4939
State[5,1]	0.3277	0.1744	0.004904	0.05391	0.3118	0.7027
State[5,2]	0.1839	0.1491	0.003809	0.006688	0.1473	0.5601
State[5,3]	0.1702	0.1423	0.003768	0.00486	0.1339	0.5251
State[5,4]	0.1629	0.1386	0.003247	0.004693	0.1261	0.52
State[5,5]	0.1554	0.1308	0.003539	0.00477	0.1198	0.4834

4.4.4 Analysis of the Blood Type AB^+ and AB^-

The AB^+ and AB^- blood groups showed comparable transitions to the B^+ and B^- blood groups (Tables 17 and 18). State [1,2] has a transition probability

of 0.3601, suggesting a 36.01% possibility of improvement for the AB^+ group, moving from a poorer stage to a better one.

Table 16: Estimated Posterior Hidden Transition Probability for Ghana Blood Type B^-

GHB-	Average	StanDev	MC_error	2.5Percent	Median	97.5 Percent
State[1,1]	0.2048	0.1411	0.004479	0.01122	0.1817	0.5298
State[1,2]	0.383	0.1701	0.005711	0.08977	0.3738	0.7314
State[1,3]	0.1247	0.1085	0.00279	0.003519	0.09511	0.3953
State[1,4]	0.1621	0.1324	0.00429	0.005402	0.1292	0.4922
State[1,5]	0.1254	0.1127	0.003581	0.003705	0.0937	0.4261
State[2,1]	0.225	0.1326	0.004298	0.03206	0.2036	0.5301
State[2,2]	0.2726	0.1448	0.004598	0.04295	0.2578	0.587
State[2,3]	0.2154	0.1308	0.004237	0.03243	0.1932	0.5231
State[2,4]	0.1814	0.1283	0.004537	0.01004	0.155	0.4931
State[2,5]	0.1056	0.09585	0.002449	0.003057	0.07852	0.3628
State[3,1]	0.15	0.127	0.003516	0.004802	0.1156	0.4635
State[3,2]	0.1428	0.1233	0.003279	0.004322	0.1097	0.4584
State[3,3]	0.2818	0.1575	0.005301	0.04286	0.2597	0.6368
State[3,4]	0.1442	0.1231	0.002993	0.00431	0.1109	0.4534
State[3,5]	0.2812	0.1553	0.004141	0.047	0.2596	0.6309
State[4,1]	0.1652	0.1391	0.00384	0.005018	0.1277	0.5142
State[4,2]	0.3444	0.1795	0.004538	0.05596	0.3272	0.7286
State[4,3]	0.1635	0.1377	0.003239	0.004175	0.1272	0.5099
State[4,4]	0.1634	0.1386	0.003918	0.00544	0.1257	0.513
State[4,5]	0.1635	0.141	0.004169	0.004556	0.1257	0.5242
State[5,1]	0.3374	0.18	0.005048	0.05555	0.3163	0.7191
State[5,2]	0.1751	0.1487	0.00424	0.005745	0.1357	0.5534
State[5,3]	0.1633	0.1401	0.003773	0.00469	0.1251	0.5187
State[5,4]	0.1624	0.1378	0.003817	0.005154	0.1273	0.514
State[5,5]	0.1619	0.1376	0.00397	0.004513	0.1261	0.5056

In general, transitions between states were smaller, ranging at 0.20 or less for AB^+ and AB^- blood types. Nonetheless, states [1,1], [2,2], and [3,3] all revealed a possibility of an infected person continuing in the same condition for people with this blood type (0.20). The analysis indicates that residents of states [4,4] and [5,5] have a lower than 0.18 probability likelihood of remaining in their respective states. these results show that this blood type exhibits the lower infection rates and movement among the various states. The transition probabilities between various states for the AB^+ and AB^- blood groups were analyzed, revealing interesting

patterns. For the AB^+ blood group, the transition from state [1,2] had the highest probability at 0.3601 (0.36), indicating a moderate chance of improving from a worse state to a better one. In contrast, transitions for this group generally ranged at or below 0.20, suggesting smaller shifts between states. Notably, states [1,1], [2,2], and [3,3] exhibited a 0.20 probability of individuals staying in the same state, while states [4,4] and [5,5] showed a less than 0.18 probability of remaining unchanged, indicating lower movement and lower infection rates in these categories. For the AB^- blood group, the transition from state [1,1] showed a higher probability of 0.4565 (0.4565), suggesting a stronger likelihood of remaining in the same state. Meanwhile, the transitions for other states were generally lower, with probabilities under 0.20. In particular, state [1,5] had the lowest probability (0.0961), and state [5,5] had a transition probability of 0.1654, showing that individuals in the AB^- group were more likely to remain in a stable state, similar to the AB^+ group. However, the analysis indicates that the AB^+ group experiences slightly more movement compared to the AB^- group, with both blood types showing relatively lower infection rates.

5 Discussion

The results from this study, based on Hidden Markov Chain (HMC) analysis, provide compelling evidence that blood type significantly influences the progression and recovery of infections. This has important clinical implications, particularly in how different blood types may respond to infectious diseases, potentially informing treatment strategies and intervention approaches.

Blood Type O^+ and O^-

Individuals with blood type O^+ show a favorable infection progression, as indicated by their higher transition probabilities from severe infection states to milder ones. Notably, the probability of transitioning from state $[5, 1]$ (most severe) to $[1, 1]$ (least severe) is 0.3634, the highest among all blood types. This suggests that O^+ individuals are more likely to recover from severe stages of infection and may experience a faster and more efficient healing process. The transition probabilities from states $[1, 2]$ (mild to moderate) and $[4, 2]$ (severe to moderate) also support this notion, suggesting that individuals with this blood type tend to stabilize and recover more easily compared to those with other blood types. Clinically, this may indicate that O^+ individuals require less intensive medical intervention, as they are more likely to improve on their own.

Table 17: Estimated Posterior Hidden Transition Probability for Ghana Blood Type AB^+

GHAB+	Average	StanDev	MC_error	2.5Percent	Median	97.5 Percent
State[1,1]	0.2724	0.1819	0.01244	0.01668	0.2387	0.6618
State[1,2]	0.3601	0.1815	0.01071	0.05732	0.3507	0.7241
State[1,3]	0.1297	0.1103	0.003136	0.004129	0.1008	0.4083
State[1,4]	0.1277	0.113	0.003514	0.004046	0.09585	0.4198
State[1,5]	0.1101	0.1006	0.003097	0.002657	0.08231	0.3651
State[2,1]	0.2061	0.1327	0.005053	0.01719	0.1823	0.5132
State[2,2]	0.2589	0.1481	0.005294	0.03718	0.2369	0.5923
State[2,3]	0.1938	0.128	0.00462	0.01464	0.1724	0.4972
State[2,4]	0.1987	0.1334	0.004583	0.01386	0.1749	0.5056
State[2,5]	0.1425	0.1347	0.008162	0.003556	0.1015	0.5099
State[3,1]	0.1766	0.1571	0.008396	0.005219	0.1306	0.5891
State[3,2]	0.1567	0.1305	0.002856	0.004712	0.1233	0.4857
State[3,3]	0.2591	0.1601	0.006837	0.02095	0.2386	0.6209
State[3,4]	0.1452	0.127	0.003284	0.004155	0.1085	0.4748
State[3,5]	0.2623	0.1644	0.006141	0.02058	0.2378	0.6301
State[4,1]	0.174	0.1518	0.005546	0.004444	0.1312	0.5617
State[4,2]	0.3264	0.1876	0.007818	0.0299	0.3117	0.7149
State[4,3]	0.1634	0.1425	0.003735	0.004691	0.1235	0.5328
State[4,4]	0.1664	0.1405	0.00453	0.005326	0.1296	0.5174
State[4,5]	0.1697	0.1426	0.004171	0.005417	0.1318	0.5296
State[5,1]	0.3432	0.1804	0.004899	0.05494	0.3263	0.7222
State[5,2]	0.1704	0.1424	0.003399	0.00535	0.1327	0.5222
State[5,3]	0.1577	0.134	0.003464	0.004972	0.1211	0.4933
State[5,4]	0.1638	0.1397	0.003546	0.004949	0.1264	0.5127
State[5,5]	0.1649	0.1388	0.004525	0.004569	0.128	0.5164

In stark contrast, individuals with blood type O^- have lower probabilities of transitioning to milder infection states, with a transition probability of 0.5132 from state $[1, 1]$ (severe) to the same state, suggesting a higher likelihood of remaining in severe stages of infection. This is indicative of a more challenging disease course for O^- individuals, who may face prolonged illness and a greater risk of deterioration. These individuals may require more intensive and proactive medical management to prevent complications. The findings imply that early intervention and close monitoring are crucial for this group, as their transition probabilities suggest a reduced likelihood of spontaneous recovery.

Table 18: Estimated Posterior Hidden Transition Probability for Ghana Blood Type AB^{-}

GHAB-	Average	StanDev	MC_error	2.5Percent	Median	97.5 Percent
State[1,1]	0.4565	0.1913	0.01119	0.04896	0.4747	0.7834
State[1,2]	0.1692	0.1364	0.006112	0.007977	0.134	0.5246
State[1,3]	0.1349	0.1096	0.004052	0.005732	0.1098	0.4127
State[1,4]	0.1434	0.1183	0.005767	0.005092	0.1144	0.4429
State[1,5]	0.09609	0.08981	0.002818	0.00259	0.06915	0.3344
State[2,1]	0.1837	0.1528	0.005676	0.006159	0.1428	0.5733
State[2,2]	0.2753	0.1719	0.007237	0.01772	0.254	0.6554
State[2,3]	0.1913	0.1506	0.006208	0.006659	0.1552	0.5571
State[2,4]	0.1539	0.1336	0.004569	0.004862	0.1173	0.4994
State[2,5]	0.1958	0.1571	0.007056	0.006017	0.1579	0.5788
State[3,1]	0.2301	0.1817	0.009346	0.007574	0.1848	0.6637
State[3,2]	0.1718	0.1464	0.004509	0.005039	0.1327	0.5434
State[3,3]	0.2142	0.1596	0.006764	0.008129	0.1818	0.581
State[3,4]	0.1609	0.1411	0.003637	0.004101	0.1233	0.5246
State[3,5]	0.223	0.164	0.007258	0.008772	0.1923	0.6185
State[4,1]	0.2455	0.1821	0.006718	0.008622	0.2118	0.6646
State[4,2]	0.2381	0.1791	0.00625	0.007577	0.2031	0.6552
State[4,3]	0.1801	0.1493	0.00415	0.004795	0.1414	0.5458
State[4,4]	0.1654	0.1373	0.003879	0.00523	0.1301	0.515
State[4,5]	0.171	0.1467	0.004202	0.005473	0.1314	0.5444
State[5,1]	0.3354	0.1841	0.00503	0.0391	0.3167	0.7206
State[5,2]	0.1753	0.152	0.004673	0.004829	0.1322	0.5658
State[5,3]	0.1647	0.1392	0.003445	0.005226	0.1279	0.5158
State[5,4]	0.1591	0.1367	0.003345	0.004613	0.1208	0.5075
State[5,5]	0.1654	0.14	0.004374	0.004893	0.1291	0.518

Blood Type A^{+} and A^{-}:

Blood types A^{+} and A^{-} show a general tendency toward stable infection states, with transition probabilities indicating more favorable outcomes for A^{+}. The transition from state $[1,1]$ (severe) to $[1,2]$ (mild to moderate) for A^{+} individuals, with a probability of 0.3961, is notably higher than for other blood types, suggesting that they are more likely to recover or stabilize during the infection. The relatively lower probabilities of deterioration to more severe states imply that individuals with blood type A^{+} may exhibit a higher baseline resilience, making them more resistant to deterioration during an infection. In contrast, A^{-} individuals show some variability in health outcomes, with a greater range of transition

probabilities. While the transition from state $[1, 1]$ to $[1, 2]$ is relatively high at 0.3764, there is greater uncertainty in the recovery process, suggesting that individuals with A^- may experience a broader spectrum of responses, ranging from recovery to deterioration. As a result, treatment for A^- individuals may need to be more tailored, considering the variability in their response to infection.

Blood Type B^+ and B^-:

For individuals with blood types B^+ and B^-, the study finds that early intervention plays a crucial role in improving health outcomes. While the probability of transitioning to state 5 (the most severe state) is relatively low, individuals in these blood groups may still face a 30% chance of deterioration into worse conditions if not properly managed. However, there is a strong probability of improvement for most individuals, with dominant transitions to state $[1, 2]$ (mild to moderate), with transition probabilities of 0.4009 for B^+ and 0.3830 for B^-. This suggests that with timely medical intervention, individuals with these blood types are more likely to recover or stabilize. The observed statistical uncertainty in the model indicates that while improvement is likely for a majority of B^+ and B^- individuals, some level of variability in outcomes exists. This uncertainty highlights the importance of monitoring patients closely and adjusting treatment plans as necessary.

Blood Type AB^+ and AB^-:

Individuals with AB^+ and AB^- blood types exhibit lower probabilities of deterioration, indicating more stable infection states. For example, the highest transition probability for the AB^+ group is 0.3601, transitioning from state $[1, 2]$ to a better condition, suggesting that these individuals have a moderate chance of improving. However, the overall probabilities of movement between states are lower for AB^+ and AB^-, indicating that these individuals are less likely to experience severe fluctuations in their health state. This stability may reflect lower infection rates and less aggressive progression of the disease in these groups. Moreover, both blood types show a reduced likelihood of remaining in the most severe states, with transition probabilities of less than 0.18 for states $[4, 4]$ and $[5, 5]$, highlighting a relatively more favorable prognosis.

Implications for Clinical Practice

The findings from this study suggest that blood type plays a significant role in influencing infection outcomes, underscoring the need for personalized treatment strategies. For blood type O^+ individuals, less intensive treatment may be

warranted due to their higher likelihood of recovery. In contrast, individuals with blood type O^- require closer monitoring and more aggressive treatment to prevent deterioration. Blood types A^+ and B^+, as well as their negative counterparts, demonstrate varied yet significant responses, suggesting that treatment strategies should be flexible and adaptive. Personalized care, based on blood type, can therefore optimize recovery rates and reduce complications.

5.1 Conclusion and Future Directions

The study found that blood types $A^+, A^-, B^+, B^-, AB^+, O^+$, and O^- may be classified into five (5) states, with the exception of $AB-$, which is classified into four states. The findings also highlight the need to consider blood type alongside other known risk factors, such as age, pre-existing conditions, and vaccination status, in predicting infection outcomes. Incorporating blood type into predictive models could improve disease management and outcome predictions, facilitating more personalized care approaches.This study highlights the importance of blood type in infection progression and recovery. The variability in transition probabilities between blood types provides valuable insights into how individuals may respond to infection, allowing for more targeted treatment strategies. As such, blood type should be considered a key factor when managing infectious diseases, guiding healthcare providers in making more informed decisions about patient care and treatment plans. While the results provide important insights into the potential influence of blood type on infection progression, further studies are needed to validate these findings across different populations. Additionally, research into the biological mechanisms underlying the observed differences between blood types could provide deeper understanding into the immune responses that influence disease severity and recovery. Future work should also explore how blood type interacts with other factors to offer more comprehensive predictions for individual disease outcomes.
While the results provide important insights into the potential influence of blood type on infection progression, further studies are needed to validate these findings across different populations. Additionally, research into the biological mechanisms underlying the observed differences between blood types could provide deeper understanding into the immune responses that influence disease severity and recovery. Future work should also explore how blood type interacts with other factors to offer more comprehensive predictions for individual disease outcomes.

References

E. Ackermann, C. T. Kemere, and J. P. Cunningham. Unsupervised clusterless decoding using a switching poisson hidden markov model. *bioRxiv*, pages 1–23, 2019. doi: 10.1101/760470.

B. Alafchi, S. Yazdi-Ravandi, R. Najafi-Vosough, A. Ghaleiha, and M. Sadeghifar. Forecasting new cases of bipolar disorder using poisson hidden markov model. *International Clinical Neuroscience Journal*, 5(1):7, 2018.

S. G. . W. N. Baum L. E., Petrie T. A maximization technique occurring in the statistical analysis of probabilistic functions of markov chains. *The Annals of Mathematical Statistics*, 41(1):164–171, 1966.

. R. C. E. Beal M. J., Ghahramani Z. The infinite hidden markov model. *Advances in neural information processing systems*, pages 577–584, 2002.

M. Castillo-Riquelme, Z. Chalabi, J. Lord, F. Guhl, D. Campbell-Lendrum, C. Davies, and J. Fox-Rushby. Modelling geographic variation in the cost-effectiveness of control policies for infectious vector diseases: The example of Chagas disease. *Journal of Health Economics*, 27(2):405–426, 2008. ISSN 01676296. doi: 10.1016/j.jhealeco.2007.04.005.

J. M. I. . W. A. S. Fox E. B., Sudderth E. B. Bayesian nonparametric inference of switching dynamics in complex systems. *Proceedings of the National Academy of Sciences*, 112(3):2014–2021, 2015.

Z. K. Gang Q, Zhou F. Hidden markov models (hmms) for medical applications. *Journal of Oncology Research Treatment*, 9(S1):1–7, 2024.

. J. M. I. Ghahramani Z. Factorial hidden markov models. *Journal of Machine learning*, 29(2-3):245–273, 1997.

M. J. Johnson and A. S. Willsky. Bayesian Nonparametric Hidden Semi-Markov Models. 14:673–701, 2013.

M. D. King, S. Pujar, and R. C. Scott. A hidden Markov model analysis of subject-specific seizure time-series data as a potential aid to clinical decision making. *F1000Research*, 5(May):2592, 2016. ISSN 2046-1402. doi: 10.12688/f1000research.9746.1.

V. Koerniawan, N. Sunusi, and R. Raupong. Estimasi Parameter Model Poisson Hidden Markov Pada Data Banyaknya Kedatangan Klaim Asuransi Jiwa. *ESTIMASI: Journal of Statistics and Its Application*, 1(2):65, 2020. ISSN 2721-3803. doi: 10.20956/ejsa.v1i2.9302.

Y. J. . W. D. Li Y., Lu H. A hidden markov model-based framework for disease progression modeling. *BMC Bioinformatics*, 17(Suppl 7):247, 2016.

. S. W. Liao Y., Smyth G. K. The r package rmixmod for (mixture model) clustering, classification, and density estimation. *Journal of Statistical Software*, 86 (6):1–30, 2018.

G. Luo, F. L. Nkoy, P. H. Gesteland, T. S. Glasgow, and B. L. Stone. A systematic review of predictive modeling for bronchiolitis. *International Journal of Medical Informatics*, 83(10):691–714, 2014. ISSN 13865056. doi: 10.1016/j.ijmedinf.2014.07.005.

B. A. Z. L. B. D. Mielke N, Gorz R. Association between abo blood type and coronavirus disease 2019 severe outcomes across dominant variant strains. *Journal of American College Emergency Physicians Open*, 5(1):1–10, 2024.

J. Murakami. Bayesian posterior mean estimates for Poisson hidden Markov models. *Computational Statistics and Data Analysis*, 53(4):941–955, 2009. ISSN 01679473. doi: 10.1016/j.csda.2008.11.012.

C. F. Nam, J. A. Aston, and A. M. Johansen. Parallel sequential Monte Carlo samplers and estimation of the number of states in a Hidden Markov Model. *Annals of the Institute of Statistical Mathematics*, 66(3):553–575, 2014. ISSN 15729052. doi: 10.1007/s10463-014-0450-4.

R. L. R. A tutorial on hidden markov models and selected applications in speech recognition. *Proceedings of the IEEE*, 77(2):257–286, 1989.

J. D. Raffa. Multivariate Longitudinal Data Analysis with Mixed Effects Hidden Markov Models by. 2012.

S. Rojas-Salazar, E. M. Schliep, C. K. Wikle, and M. Hawkey. A bayesian hidden semi-markov model with covariate-dependent state duration parameters for high-frequency data from wearable devices. *arXiv preprint arXiv:2010.10739*, pages 1–27, 2020.

S. P. Sarode Rekha, Tirupathi Rao Padib. Markov modelling of t2dm progression. *Journal Of Statistics, Optimization And Data Science*, 1(2):10–21, 2023.

L. Shaochuan. A Bayesian multiple changepoint model for marked poisson processes with applications to deep earthquakes. *Stochastic Environmental Research and Risk Assessment*, 33(1):59–72, 2019. ISSN 14363259. doi: 10.1007/s00477-018-1632-z. URL `https://doi.org/10.1007/s00477-018-1632-z`.

X. Song, K. Kang, M. Ouyang, X. Jiang, and J. Cai. Bayesian Analysis of Semiparametric Hidden Markov Models With Latent Variables. *Structural Equation Modeling*, 25(1):1–20, 2018. ISSN 15328007. doi: 10.1080/10705511.2017.1364968.

N. S. C. K. K. P. W. L. W. M. D. J. H. S. H. J. K. D. M. D. R. P. Soper BC, Cadena J. Dynamic modeling of hospitalized covid-19 patients reveals disease state-dependent risk factors. *J Am Med Inform Assoc.*, 29, 2022.

W. Su and X. Wang. Hidden Markov model in multiple testing on dependent count data. *Journal of Statistical Computation and Simulation*, 90(5):889–906, 2020. ISSN 15635163. doi: 10.1080/00949655.2019.1710507. URL `https://doi.org/00949655.2019.1710507`.

S. M. . G. T. L. Tran T., Turner R. E. Hierarchical dirichlet processes. *Journal of Machine Learning Research,*, 17(1), 2016.

Y. B. L. Y. Y. J. C. H. X. Z. X. K. Wei Zhang, Caiping Zhang. Analysis of covid-19 epidemic and clinical risk factors of patients under epidemiological markov model. *Results in Physics*, 22, 2021.

. D. Z. Y. Zhang Y., Wu S. Hidden markov model-based financial time series prediction. *Entropy*, 21(6):585, 2019.

W. Zucchini, I. L. MacDonald, R. Langrock, W. Zucchini, I. L. MacDonald, and R. Langrock. Preliminaries: mixtures and Markov chains. *Hidden Markov Models for Time Series*, (July 2007):3–28, 2018. doi: 10.1201/b20790-1.